

(RESEARCH ARTICLE)



## Structural and molecular modifications of woody biomass under minimal torrefaction conditions toward making durable pellets

Kanageswari Singara veloo<sup>\*</sup>, Anthony K Lau and Shahabaddine Sokhansanj

*Biomass and Bioenergy Research Group, Department of Chemical and Biological Engineering, University of British Columbia, Vancouver, B.C., Canada.*

GSC Advanced Research and Reviews, 2024, 20(03), 129–138

Publication history: Received on 02 August 2024; revised on 16 September 2024; accepted on 18 September 2024

Article DOI: <https://doi.org/10.30574/gscarr.2024.20.3.0341>

### Abstract

Extensive research has been published on pelletizing severely torrefied biomass with the aid of binders, but limited studies have investigated the structural modifications of biomass during mild torrefaction. This study investigates the effects of several combinations of minimal torrefaction temperatures (230°C and 250°C) and relatively short durations (10, 15, and 30 minutes) on the thermophysical and molecular structure of the model woody biomass loblolly pine (*Pinus Taeda*) residues. The low severity treated biomass is compared with the untreated biomass and the biomass torrefied at 270°C for 30 minutes. Structural characterization methods include laser diffraction for particle size distribution and Brunauer-Emmett-Teller (BET) analysis to evaluate specific surface area. Additionally, FTIR, XRD, and TGA are used to assess changes in crystallinity and thermochemical composition. The woody residue torrefied at 250°C for 10 minutes exhibited a higher BET surface area (4.7 m<sup>2</sup>/g) than torrefied at 250°C for 15 minutes (3.5 m<sup>2</sup>/g). At a constant temperature of 250°C, the crystallinity index increases with the treatment duration, emphasizing the effect of time on retaining more hydroxyl groups that may act as binders for pelletization. This study demonstrates that minimizing the combination of torrefaction time and temperature can help control the degree of biomass molecular structure degradation thus minimizing overall mass loss, offering potential applications in the emerging biocarbon pellet industry.

**Keywords:** Woody biomass; Minimal torrefaction; Binding properties; Molecular modification; Physical structure of particles

### 1. Introduction

Biomass-based energy production is offered as a potential solution to diverting from fossil fuel energy production [1]. However; biomass resources are difficult to handle; transport; store; and utilize in their original form due to their high moisture or ash content; lower heating value and irregular shape and sizes [2;3]. Additionally; the seasonality and the long distances between biomass production sites; such as forests and agricultural lands; and industrial or residential areas requiring substantial logistics for transportation and storage [3;4]. To address these challenges; biomass can undergo a thermal pre-treatment process known as torrefaction; combined with pelletization; resulting in a high-energy-density; brittle solid fuel that can serve as a viable coal substitute [5–7].

Lignocellulosic biomass is composed of cellulose; lignin; and hemicellulose; along with other molecules known as extractives [4;5]. Torrefaction involves heating biomass at 200–300°C in limited oxygen conditions; which removes moisture and partially decomposes the material [8]. Light torrefaction occurs within the temperature range of 200°C to 240°C; where hemicellulose degradation initiates [3]. Increasing temperature to 240°C to 260°C degrades hemicellulose to a greater extent; while severe torrefaction occurs between 260°C to 300°C; leading to the depolymerization of cellulose; hemicellulose; and lignin molecules [4;9]. The mechanical compression of torrefied biomass results in a

<sup>\*</sup> Corresponding author: Kanageswari Singaraveloo

second-generation pellets offering a product with higher energy density; reduced handling and storage costs; and improved stability compared to raw biomass pellets [10;11].

Several studies have examined the characteristics of torrefied biomass prior to pelletization over a wide range of treatment temperatures and residence times [10;12–17]. Compared to pellets made from untreated biomass; torrefied biomass tends not to bind because torrefaction degrades lignin molecules and weakens particle bonding [5;6;13;14;18]. Severe torrefaction further compromises these properties; making pelletization more challenging [5;6;18]. The critical review of literature performed by Igalavithana et al. [19] highlighted the diversity of molecular compositions among lignocellulosic biomass and the need for understanding the structural modifications of a specific biomass species upon its torrefaction [15].

Thermogravimetric analysis (TGA) is commonly used to assess thermal decomposition; while other advanced analytical instruments like Fourier Transform Infrared (FTIR) spectroscopy and X-ray diffraction (XRD) provide insights into surface functional groups and crystallinity [20;21]. It has been reported that significant changes occurred in the FTIR spectra between 1200-800  $\text{cm}^{-1}$  and the XRD peak intensities of the amorphous and crystalline cellulose ( $\sim 16^\circ$  and  $22^\circ$ ) due to torrefaction treatment; which affected the polysaccharides; mainly hemicellulose and cellulose characteristics [21]. These detailed analyses are crucial for illustrating how the molecular structures and their functionality influence the binding properties of the biomass.

The motivation for the current research came from an inquiry on whether woody biomass from loblolly pine can be minimally torrefied to make pellets without the use of binders. The objective is to minimize mass loss while still gaining some of the benefits of torrefaction; such as hydrophobicity and an increase in calorific value. To the best of our knowledge; the thermal; physical; and molecular changes that occur in torrefied loblolly pine (*Pinus Taeda*) residues; especially in the context of their use as a feedstock for pelletization; have not been published in the open literature. A series of controlled experiments are undertaken to expose the as received ground loblolly pines to minimal thermal treatments. The treated biomass is then subject to compaction and densification. This paper presents the data and analysis of the treated biomass prior to pelletization. The properties of torrefied pellets will be presented in a subsequent publication.

## 2. Material and methods

### 2.1. Materials

Samples of Loblolly pine (*Pinus taeda*); are received from the industrial partner in the form of ground samples. The as received moisture content of the samples averaged 9.0 wt%. Before undergoing torrefaction; the collected biomass is dried in a convection oven at  $105^\circ\text{C}$  for 24 h. The dried material is sealed in a glass jar until use.

### 2.2. Torrefaction

The torrefaction experiment is conducted using an in-house built thin-layer thermogravimetric analyzer (macro TGA) shown in Figure 1 [22]. A consistent mass of approximately 10-15 grams of biomass feedstock is utilized for all the experiments. A continuous nitrogen gas flow rate of 50 mL/min is maintained inside the macro TGA unit to ensure an inert atmosphere. The torrefaction is conducted at 230; 250; and  $270^\circ\text{C}$  with varying residence times of 10; 15; and 30 minutes. The mass yield; energy density and energy yield for each torrefied sample at different conditions are calculated as follows [17]:

$$\text{Mass Yield (MY)} = \left( \frac{\text{mass}_{\text{dry basis torrefied}}}{\text{mass}_{\text{dry basis untreated}}} \right) \times 100 \quad 1$$

$$\text{Energy Density (ED)} = \frac{\text{HHV}_{\text{torrefied}}}{\text{HHV}_{\text{untreated}}} \quad 2$$

$$\text{Energy Yield} = \text{MY} \times \text{ED} \times 100 \quad 3$$

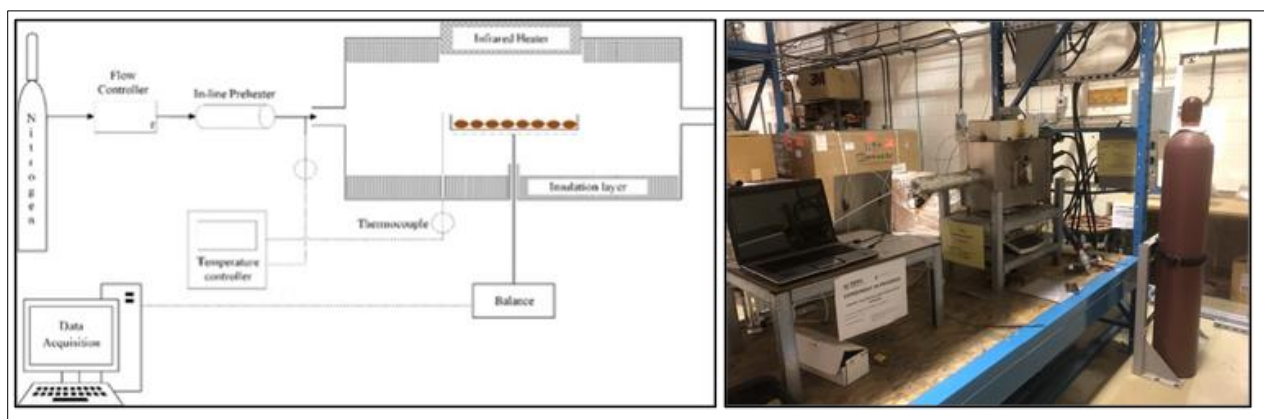


**Figure 1** Schematic diagram (left) and setup (right) of the macro TGA unit [22]

### 2.3. Measurements

Measurements are made on both bulk and single particles. The ASTM D1755-01 standard is followed to conduct the proximate analysis of biomass before and after treatment that determines the volatile content; and ash content while the fixed carbon is calculated by difference. Volatile content is measured through thermogravimetric treatment at 950°C in oxygen-free environment for 10 minutes. Ash content is obtained by burning particles in dry air at 575°C for 6 hours; calculating dry-basis ash content. The higher heating value (HHV) of the sample before and after treatment is determined using an oxygen bomb calorimeter (Parr Model 6100). To ensure the reliability of the results; all analyses are performed thrice. The ultimate analysis is carried out separately using a Fisons-EA 1108 elemental analyzer (Thermo Scientific; USA) to measure the weight percentages of C; H; and N in samples; while the oxygen content is calculated by difference.

Bulk density is measured using the method used by Yu et al. [23] for ground cellulosic biomass. A 25 mL glass cylinder (25.4 mm diameter) is filled with biomass; which is freely poured from a height of 200 mm. Excess material is levelled off with a rubber-coated rod. Bulk density is calculated as the ratio of the sample mass to its occupied volume. A Malvern Mastersizer equipment; Series 2000 (Malvern-Panalytical; United Kingdom) equipped with a dry measurement module (Scirrocco series) is used to determine mass median diameter  $d[0.5]$  and the size of particle below which 10% and 90% of the sample lies;  $d[0.1]$  and  $d[0.9]$ ; respectively for materials before and after treatment. The equipment used a laser diffraction technique for size measurements in the range of 0.02–2000  $\mu\text{m}$ . A tablespoon (a few grams) of particles is analyzed three times. The BET method is used to determine the surface area using the Sync 400 (Altamira Instrument; USA). Samples are degassed under vacuum at 105°C for 15 h prior to gas sorption experiments. For the analysis; the samples are cooled to -196°C using a liquid nitrogen bath; which is also employed as the adsorption gas.

Fourier transform infrared spectroscopy (Bruker Inventio ATR-FTIR spectrometer; Germany) is used to characterize the changes of the typical functional groups of untreated and treated samples. Attenuated total reflectance (ATR) mode is used for recording the spectra (4500-400  $\text{cm}^{-1}$ ).

For the collection of X-ray diffraction (XRD) data; diffraction patterns are obtained using an Empyrean 3 X-ray diffractometer (Malvern-Panalytical; United Kingdom) equipped with copper radiation ( $\lambda = 0.155418 \text{ nm}$ ). The instrument is operated at a voltage of 45 kV and a current of 40 mA. The  $2\theta$  range from 5° to 50° is measured and compared with XRD data from the literature obtained using a copper target. The crystallinity index ( $CrI$ ) is determined using the peak-height method [16;23] in equation 4; while the crystallite sizes of the samples are calculated using the Debye-Scherrer equation in equation 5 [16;24].

$$CrI (\%) = \frac{I_{200} - I_{110}}{I_{200}} \times 100 \quad 4$$

where  $I_{200}$  is the maximum intensity above baseline at  $2\theta = 22^\circ$  and  $I_{110}$  is the minimum intensity above baseline corresponding to amorphous content at  $2\theta = 16^\circ$ .

$$D = \frac{0.9\lambda}{\beta \cos\theta} \quad 5$$

where  $\lambda$  is the wavelength of the X-ray beam;  $\beta$  denotes the full width at half maximum (FWHM) in radians;  $\theta$  is the scattering angle and  $D$  is the crystallite size (nm).









Thermogravimetric analysis is performed using a thermogravimetric analyzer; TGA (Model Q550) under nitrogen environment (TA Instruments; Germany). About 10 mg of sample is used in each run. The decomposition behavior is investigated by the following steps [23]: (1) a heating rate of 20°C/min from ambient temperature to 105°C; (2) isothermal for 10 min; (3) a heating rate of 20°C/min from 105°C to 800°C; (4) isothermal for 10 min.

### 3. Result and Discussion

#### 3.1. Torrefaction

Table 1 lists treatment conditions and the relevant data for the untreated and treated biomass. The experimental data include the proximate and ultimate analyses for untreated and treated loblolly pine at a low severity of 230-270°C and 10-30 minutes. The volatile matter decreases from 81.0 wt% for the untreated to 67.9 wt% for the most severe treatment at 270°C; 30 min. The fixed carbon shows an increasing trend from 18.7 wt% to 31.5 wt% as the severity of treatment increased. Those results are in line with Yang et al. [25] who reviewed and compiled the organic component composition and elemental distribution in torrefied biomass. At higher torrefaction temperatures and longer residence times; a significant upward trend in ash content from 0.40 wt% for 230°C;10 min to a high of 0.87% at 250°C;15 min is observed. This increase is attributed to the breakdown of carbon-hydrogen bonds; resulting in volatile loss and a subsequent concentration of ash in the biomass [26].

**Table 1** Properties of untreated and torrefied loblolly residue. The values are reported as average  $\pm$  standard deviation. Asterisks (\*) is used to denote the statistical significance differences between the untreated and treated material properties using t-test (assume equal variances and alpha value is 0.05)

| Treatment (°C; minute)              | Untreated   | 230;10  | 230;15  | 230;30  | 250;10   | 250;15  | 250;30  | 270;30  |
|-------------------------------------|---|---|---|---|--|---|---|---|
|                                     |  |  |  |  |  |  |  |  |
| Proximate analysis (wt.%;dry basis) |   |   |   |   |  |   |   |   |
| Volatile content (n=3)              | 81.0 $\pm$ 0.01   | 79.65 $\pm$ 0.45*   | 79.26 $\pm$ 0.21*   | 78.10 $\pm$ 0.38*   | 78.65 $\pm$ 0.15*  | 76.87 $\pm$ 0.19*   | 75.08 $\pm$ 1.45*   | 67.88 $\pm$ 0.79*   |
| Fixed carbon (n=3)                  | 18.71 $\pm$ 0.14  | 20.0 $\pm$ 0.46*  | 20.46 $\pm$ 0.29*   | 21.38 $\pm$ 0.39*   | 21.01 $\pm$ 0.04*  | 22.47 $\pm$ 0.56*   | 24.29 $\pm$ 1.29*   | 31.47 $\pm$ 0.53*   |
| Ash (n=3)                           | 0.35 $\pm$ 0.14   | 0.40 $\pm$ 0.10   | 0.36 $\pm$ 0.14   | 0.49 $\pm$ 0.06   | 0.34 $\pm$ 0.12  | 0.87 $\pm$ 0.44   | 0.63 $\pm$ 0.12   | 0.65 $\pm$ 0.26   |
| Elemental analysis (wt.%;dry basis) |   |   |   |   |  |   |   |   |
| C (n=2)                             | 46.66 $\pm$ 2.15  | 47.69 $\pm$ 1.62  | 49.68 $\pm$ 0.0   | 50.55 $\pm$ 0.45  | 49.72 $\pm$ 0.33   | 52.16 $\pm$ 0.31  | 55.34 $\pm$ 0.45*   | 56.84 $\pm$ 2.33*   |
| H (n=2)                             | 5.61 $\pm$ 0.30   | 6.02 $\pm$ 0.0  | 6.09 $\pm$ 0.23   | 5.89 $\pm$ 0.05   | 5.98 $\pm$ 0.34  | 6.02 $\pm$ 0.04   | 5.85 $\pm$ 0.01   | 5.65 $\pm$ 0.08   |
| O <sup>a</sup>                      | 47.38   | 45.89   | 43.87   | 43.07   | 43.96  | 40.95   | 38.18   | 36.86   |
| Heating value; d.b. (MJ/kg) (n=3)   | 19.54 $\pm$ 0.03  | 19.86 $\pm$ 0.02*   | 19.92 $\pm$ 0.08*   | 20.25 $\pm$ 0.10*   | 20.62 $\pm$ 0.13*  | 20.61 $\pm$ 0.02*   | 21.28 $\pm$ 0.05*   | 22.53 $\pm$ 0.23*   |
| Mass yield (%)                      | 100.0   | 92.06   | 90.34   | 88.5  | 86.18  | 84.91   | 81.61   | 62.39   |
| Energy yield (%)                    | 100.0   | 93.57   | 92.10   | 91.72   | 90.94  | 89.56   | 88.88   | 71.94   |
| Energy density                      | 1.0   | 1.02  | 1.02  | 1.04  | 1.06   | 1.05  | 1.09  | 1.15  |

<sup>a</sup> O= 100-C-H-Ash (dry basis)

A t-test with shows that values of the properties reported in Table 1 for treated biomass are all significantly ( $p=0.05$ ) different from the values for the untreated biomass. During the torrefaction process; H/C and O/C ratios decrease as the biomass loses some oxygenate and hydrogenate compounds; which densifies the carbon content [14]. This suggests a rise in the proportion of carbon that remains in the biomass after volatiles are expelled; indicating increased heating value and energy density aligning with other studies [12;14;17]. The heating value increases as the temperature rises; but there is not much noticeable difference with extended duration at the same temperature. The darkening in colour of the biomass during torrefaction is due to the removal of volatile components resulting in significant enrichment of carbon content [25].

The mass yield decreases as the torrefaction temperature and duration increase because the raw biomass is subjected to torrefaction; its dry matter reduces because of thermal breakdown [5]. The lowest mass yield was found at 270°C;30 min as severe torrefaction led to the depolymerization of cellulose; hemicellulose; and lignin [4;11]. Energy yield represents the percentage of energy retained in the biomass after torrefaction compared to the untreated biomass [17]. It decreases slightly with increasing torrefaction temperature and duration. Even though both the energy yield and mass yield decreases; the rate of decrease with temperature for energy yield is lower than the decrease for mass yield. These indicate that a minimal torrefaction positively influences the heating value but not to a great extent [17].

### 3.2. Physical structure

Table 2 shows the bulk density; size distribution; and specific surface area for untreated and treated biomass. The bulk density of the treated loblolly pine residues reduces significantly when treated at temperatures of 250°C and higher. This may be due to the fact that the torrefaction at elevated temperatures tends to break down the organized and compact lignocellulosic structure (composed of cellulose; hemicellulose; and lignin) in biomass; leading to a decrease in bulk density [14].

**Table 2** Particle size and BET total surface area of untreated and torrefied SYP

| Treatment (°C; min) | Particle size          |                        |                        | BET  | Bulk density                     |
|---------------------|------------------------|------------------------|------------------------|--|----------------------------------|
|                     | $d[0.1]$ $\mu\text{m}$ | $d[0.5]$ $\mu\text{m}$ | $d[0.9]$ $\mu\text{m}$ | Surface area ( $\text{m}^2\text{g}^{-1}$ ) | ( $\text{kg}/\text{m}^3$ ) (n=5) |
| Untreated           | 660                    | 1033                   | 1537                   | 1.01                                       | $296.8 \pm 6.6$                  |
| 230;10              | 650                    | 1008                   | 1512                   | 2.12                                       | $295.7 \pm 9.5$                  |
| 230;15              | 555                    | 915                    | 1455                   | 2.71                                       | $295.8 \pm 3.5$                  |
| 230;30              | 557                    | 902                    | 1405                   | 2.16                                       | $296.8 \pm 12.6$                 |
| 250;10              | 550                    | 895                    | 1412                   | 4.65                                       | $280.8 \pm 7.6$                  |
| 250;15              | 536                    | 822                    | 1262                   | 3.51                                       | $281.2 \pm 11.6$                 |
| 250;30              | 512                    | 846                    | 1344                   | 3.65                                       | $287.1 \pm 4.9$                  |
| 270;30              | 491                    | 789                    | 1252                   | 8.84                                       | $208.6 \pm 5.3$                  |

Upon examining the particle size; it is noticed that the mass median particle size  $d[0.5]$ ; decreases from 1033 $\mu\text{m}$  to 902 $\mu\text{m}$ ; 846 $\mu\text{m}$ ; and 789 $\mu\text{m}$ ; when compared to the untreated sample. Wang et al. [27] found a similar trend in the reduction of particle size and reasoned that this is due to the sawdust attrition during the torrefaction process. In the present case; the biomass is stationary and no attrition is involved. It is probable that the particles may have experienced shrinkage due to material loss after torrefaction [28]. Yuan et al. [29] reported a 78.4% reduction in particle size for the compost of food waste and sawdust after torrefied at 300°C for 30 mins which is 4 times higher than our result.

Medium or fine ground feed particles are desirable for pelletization because the pore spaces created by larger particles can be filled by finer particles; promoting the formation of inter-particle bonds [26]. If these fine particles deform under high pressure during pelletization; no binder is required; as the strength is provided by Van der Waals forces or particle interlocking [4]. Additionally; the size and shape of the particles determine the available surface area needed for secure bonding during pellet formation. Smaller particle sizes; in particular; offer a larger surface area; which is advantageous for creating strong bonds during pelletization [4;14].

Torrefaction at higher temperatures generally results in increased BET surface area compared to lower temperatures. For instance; at 270°C for 30 minutes; the surface area dramatically increases to 8.8 m<sup>2</sup>/g compared to 3.7 m<sup>2</sup>/g for the material treated at 250°C for 30 minutes. Varying the residence time at a specific temperature shows mixed results in surface area changes. For instance; at 230°C; increasing the residence time from 10 to 15 minutes results in a higher surface area (2.7 m<sup>2</sup>/g compared to 2.1 m<sup>2</sup>/g); but further increasing it to 30 minutes led to a slight decrease (2.2 m<sup>2</sup>/g). Similarly; at 250°C; there's a fluctuation in surface area with changing residence time.

Zheng et al. [24] reported that the specific surface area of torrefied pine particles varied with temperature over a 30-minute period. For material torrefied at 230°C; the surface area increased from 0.16 m<sup>2</sup>/g (untreated) to 50.08 m<sup>2</sup>/g; then decreased to 14.58 m<sup>2</sup>/g at 250°C; before rising again to 39.54 m<sup>2</sup>/g when torrefied at 270°C. However; before torrefaction; softwood and hardwood chips exhibited greater surface area compared to sweet sorghum bagasse; as shown in the BET study by Mafu et al [30]. Upon torrefaction; no significant changes are reported for the woody biomass; whereas sweet sorghum bagasse has shown an increase in BET surface area. Moreover; based on Ong et al. [21] review; only four studies have been reported BET method as part of the structural analysis of torrefied biomass and most of these studies concluded no significant findings in the results.

### 3.3. Changes in molecular structure

The FTIR spectra for untreated and torrefied materials are shown in Figure 2. All the materials show similar spectra except the intensities of the functional groups. The intensity of broader peaks at 3200-3400 cm<sup>-1</sup> that indicates the presence of hydroxyl (-OH) significantly decreases after evaporation; dehydration and devolatilization of volatile low-molecular weight components [21]. This peak becomes almost flat for materials torrefied above 250°C for 15 minutes. Interestingly; the band shows higher intensity for samples torrefied at 250°C for 10 minutes compared to those at 230°C for 30 minutes. This confirmed that torrefaction temperature and time can be optimized to minimize wood polymer degradation; ensuring sufficient hydroxyl groups remain on the wood polymer chains to form strong inter-particle bonds during pelletization [15].

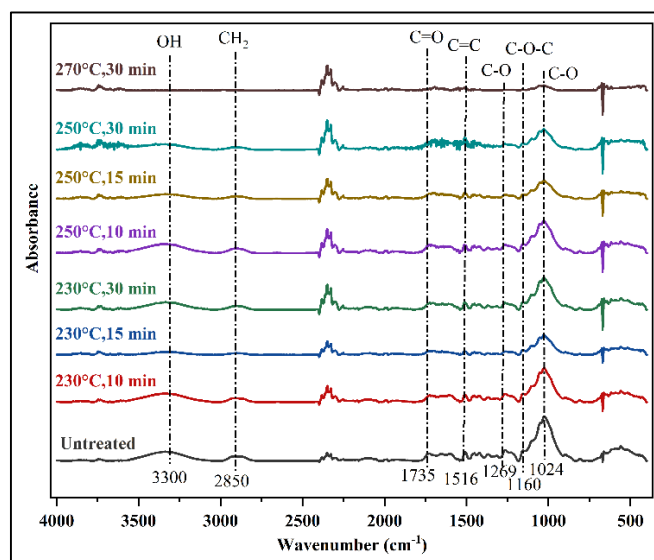


**Figure 2** FTIR spectra of untreated and torrefied materials

The reduction of the peak at 2850 cm<sup>-1</sup> shows the removal of aliphatic methylene group -CH<sub>2</sub>- in hemicellulose [31]. As a result of the acetyl group of hemicellulose removal; the signal of the unconjugated C=O vibration at 1740 cm<sup>-1</sup> diminishes with the increasing degree of torrefaction [16]. The vibrations of amorphous lignin can be attributed to the C=C stretching of the benzene ring; represented by the peak at 1540 cm<sup>-1</sup>; and the aromatic C-O stretching of methoxyl and phenylpropane units at 1269 cm<sup>-1</sup> [15;31]. The disappearance of these bands in the torrefied samples; especially at 270°C for 30 minutes; indicates the degradation of amorphous lignin under severe torrefaction conditions [21;32]. In contrast; mildly torrefied samples retain enough amorphous polymers; which can be plasticized during pelletization to form solid inter-particle bridges [15]. The cellulose antisymmetric stretching of C-O-C corresponds to the band at 1160 cm<sup>-1</sup>; with intensity decreasing as torrefaction severity increases [15]. Additionally; C-O stretching and O-H deformation in oxygen-containing organic compounds such as alcohols; phenols; and ethers diminish; as seen in the decreasing intensity of the peak at 1000 cm<sup>-1</sup> with increasing torrefaction severity [31].

X-ray diffraction (XRD) is widely used to examine the decrystallization of biomass samples after torrefaction[21]. Lignocellulose contains crystalline cellulose and amorphous cellulose; while both hemicellulose and lignin are amorphous [24]. Two major peaks corresponding to crystalline cellulose (110 and 200) are identified at diffraction angles of approximately 16° and 22° in both untreated and torrefied loblolly pine residues; as shown in Figure 3. The XRD curve for the untreated sample exhibits lesser intense peaks at these angles compared to the torrefied samples. No peak shifts are observed at either angle across the samples. Interestingly; Sarker et al. [16] reported that these peaks were very prominent in untreated canola residue; with their intensity decreasing as torrefaction severity increased. However; this finding did not align with our results.

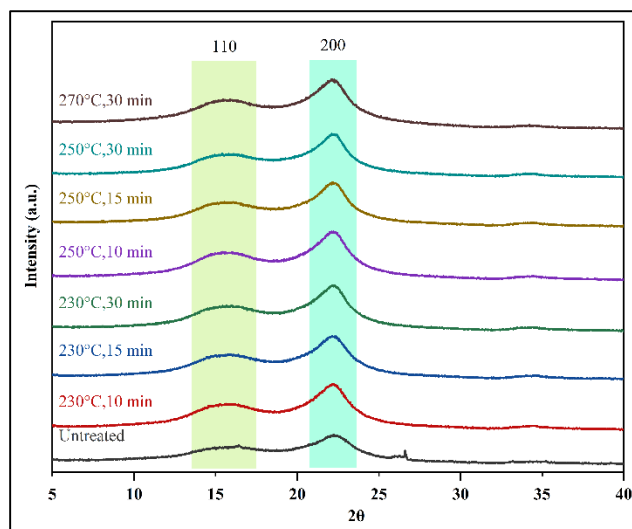


**Figure 3** X-ray diffractometry profiles of untreated and torrefied samples

The Crystallinity Index (*CrI*) for loblolly pine residues torrefied at 230°C for 10 minutes (35.9%) is slightly higher than that of untreated pine residues (31.9%). Extending the torrefaction duration at constant temperatures showed a gradual increase in *CrI* at both 230°C and 250°C. At 30 minutes; raising the temperature from 230°C to 250°C increased the *CrI* from 36.2% to 38.4%. However; further increasing the temperature to 270°C resulted in a *CrI* decrease to 34.2%; indicating severe cellulose crystallinity degradation under harsh torrefaction conditions. Gong et al. [33] observed a similar trend when torrefying pine sawdust; where *CrI* initially increased at 230°C and rose further at 260°C; attributed to the degradation of hemicellulose; which lacks crystallinity and has lower thermal stability than cellulose. The initial rise in *CrI* suggests that amorphous cellulose partially recrystallizes during torrefaction before degrading at higher temperatures [34]. Interestingly; the *CrI* for samples torrefied at 250°C for 10 minutes is lower than for those torrefied at 230°C for 30 minutes; suggesting the presence of amorphous cellulose; which can facilitate the pelletization process.

**Table 3** The crystallinity indices and crystallite sizes of the untreated and torrefied samples

| Treatment<br>(°C; min) | Crystallinity index; <i>CrI</i> ; (%) | Crystallite size (nm) |
|------------------------|---------------------------------------|-----------------------|
|                        |                                       | 200                   |
| Untreated              | 31.88                                 | 3.44                  |
| 230;10                 | 35.95                                 | 3.58                  |
| 230;15                 | 35.70                                 | 3.62                  |
| 230;30                 | 36.20                                 | 3.73                  |
| 250;10                 | 34.36                                 | 3.65                  |
| 250;15                 | 37.28                                 | 3.88                  |
| 250;30                 | 38.39                                 | 3.90                  |
| 270;30                 | 34.22                                 | 3.61                  |

Moreover; the observed increase in crystallite size in loblolly pine residues torrefied at 250°C for 15 and 30 minutes aligns with Zheng et al. [24] 's findings on the recrystallization of amorphous cellulose in biomass torrefied at the same temperature. Wang et al. [35] further support this conclusion; noting that the decomposition of amorphous cellulose becomes dominant at 250°C after 15 minutes; contributing to the increase in *Crl*.

### 3.4. Thermogravimetric analysis (TGA)

Figure 4 illustrates the thermal stability of loblolly pine residues torrefied at different temperatures for 30 minutes compared to the untreated sample. The untreated loblolly pine residues exhibit the highest weight loss; indicating the lowest thermal stability among all samples. When comparing weight loss between 230°C and 250°C; there is only a 2.2% difference. However; when the temperature is increased to 270°C; a more significant difference of 6.8% (threefold) is observed; indicating the loblolly pine residues that torrefied under severe torrefaction condition is more thermally stable.

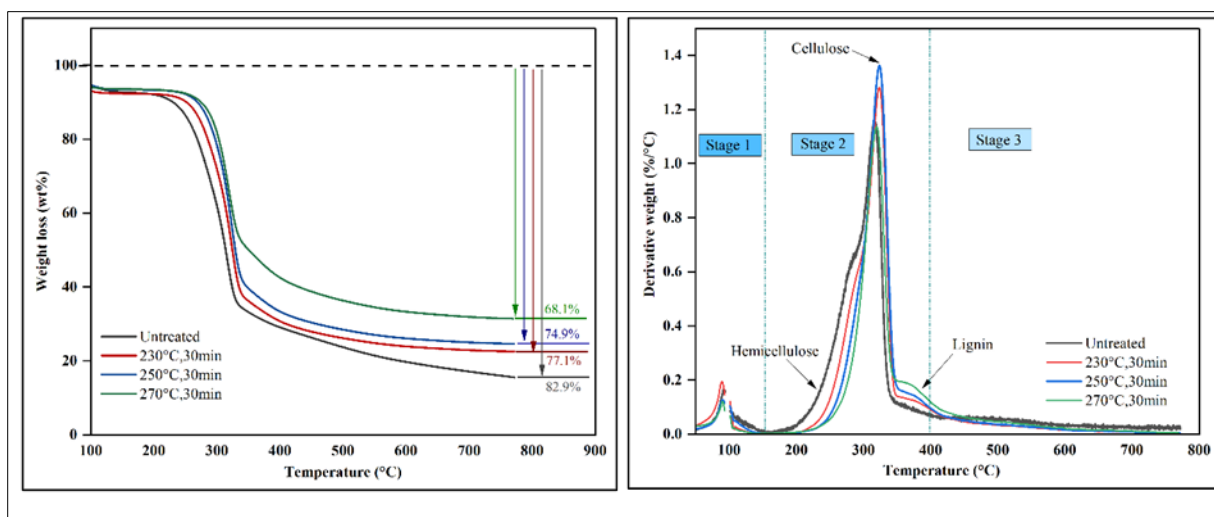


**Figure 4** Thermogravimetric (left) and differential thermogravimetric (right) analyses of selected samples

The DTG analysis graphs of untreated and torrefied loblolly pine residues reveal similar thermal degradation patterns; with three distinct regions. The first region; from 0–150°C; involved weight loss primarily due to the evaporation of free water and the release of organic substances with low boiling points. The second region; occurring between 200–400°C; is associated with the breakdown of hemicellulose and cellulose; as well as the release of volatile matter. The third region; above 400°C; represented lignin degradation. Due to its complex structure; lignin is difficult to decompose and requires higher temperatures; typically ranging from 250–500°C. Chen and Kuo [36] investigated the effects of torrefaction and co-torrefaction on hemicellulose; cellulose; and lignin at various temperatures (230°C; 260°C; and 290°C) for 1 hour; corresponding to light; mild; and severe torrefaction conditions. These two studies suggested that the thermal stability hierarchy during torrefaction is cellulose > lignin > hemicellulose; which is in line with our TGA results.

The peak intensity at 234°C marks the maximum degradation rate of hemicellulose [16]. For torrefied loblolly pine residues; the hemicellulose peaks decreased in intensity and shifted to lower temperatures; indicating significant destruction of the hemicellulose structure after torrefaction. The peak at approximately 320°C corresponds to the thermal decomposition of cellulose; and the DTG curve for loblolly pine torrefied at 270°C showed a reduced cellulose peak amplitude; indicating severe cellulose degradation. As the temperature increased; the growing amplitude of the lignin peak suggested an increase in its mass fraction; particularly at 270°C. This increase can be attributed to the severe degradation of both hemicellulose and cellulose; as previously explained. Similar findings for torrefied biomass have been reported in other studies [14;16;30;33].

## 4. Conclusion

In this study; the effects of minimal torrefaction with varying combinations of temperature and time on the thermo-physical and molecular properties of loblolly pine residues are analyzed. Torrefaction temperature has a more pronounced impact on mass yield; energy content; and both proximate and ultimate analyses compared to residence



time. The observed changes in the physical and molecular structure of the residues confirmed that optimizing torrefaction conditions can reduce wood polymer degradation while preserving hydroxyl groups essential for strong inter-particle bonding during pelletization. Additionally; DTG curves indicate an increase in lignin content after torrefaction; which could enhance pellet durability by acting as a natural binder. However; the reduction in hydrogen bonding sites may pose challenges to produce durable torrefied pellets. Overall; this study demonstrates that applying minimal torrefaction condition can preserve sufficient amorphous polymers for effective solid inter-particle bonding

---

## Compliance with ethical standards

### *Acknowledgments*

The Natural Sciences and Engineering Research Council of Canada supports this research.

### *Disclosure of conflict of interest*

No conflict of interest to be disclosed.

---

## References

- [1] Bajwa DS; Peterson T; Sharma N; Shojaeiarani J; Bajwa SG. A review of densified solid biomass for energy production. *Renew Sustain Energy Rev* 2018;96:296–305. <https://doi.org/10.1016/j.rser.2018.07.040>.
- [2] Kumar L; Koukoulas AA; Mani S; Satyavolu J. Integrating Torrefaction in the Wood Pellet Industry: A Critical Review. *Energy Fuels* 2017;31:37–54. <https://doi.org/10.1021/acs.energyfuels.6b02803>.
- [3] Stelte W; Sanadi AR; Shang L; Holm JK; Ahrenfeldt J; Henriksen UB. RECENT DEVELOPMENTS IN BIOMASS PELLETIZATION – A REVIEW. *Bioresources* 2012;7:4451–90.
- [4] Adeleke AA; Odusote JK; Ikubanni PP; Lasode OA; Malathi M; Paswan D. Essential basics on biomass torrefaction; densification and utilization. *Int J Energy Res* 2021;45:1375–95. <https://doi.org/10.1002/er.5884>.
- [5] Thengane SK; Kung KS; Gomez-Barea A; Ghoniem AF. Advances in biomass torrefaction: Parameters; models; reactors; applications; deployment; and market. *Prog Energy Combust Sci* 2022;93:101040. <https://doi.org/10.1016/j.pecs.2022.101040>.
- [6] Manouchehrinejad M; Mani S. Torrefaction after pelletization (TAP): Analysis of torrefied pellet quality and co-products. *Biomass Bioenergy* 2018;118:93–104. <https://doi.org/10.1016/j.biombioe.2018.08.015>.
- [7] Tumuluru JS; Ghiasi B; Soelberg NR; Sokhansanj S. Biomass Torrefaction Process; Product Properties; Reactor Types; and Moving Bed Reactor Design Concepts. *Front Energy Res* 2021;9:728140. <https://doi.org/10.3389/fenrg.2021.728140>.
- [8] Peng J; Wang J; Bi XT; Lim CJ; Sokhansanj S; Peng H; et al. Effects of thermal treatment on energy density and hardness of torrefied wood pellets. *Fuel Process Technol* 2015;129:168–73. <https://doi.org/10.1016/j.fuproc.2014.09.010>.
- [9] Mohammadi A. Overview of the Benefits and Challenges Associated with Pelletizing Biochar. *Processes* 2021;9:1591. <https://doi.org/10.3390/pr9091591>.
- [10] Li H; Liu X; Legros R; Bi XT; Jim Lim C; Sokhansanj S. Pelletization of torrefied sawdust and properties of torrefied pellets. *Appl Energy* 2012;93:680–5. <https://doi.org/10.1016/j.apenergy.2012.01.002>.
- [11] Chen W-H; Peng J; Bi XT. A state-of-the-art review of biomass torrefaction; densification and applications. *Renew Sustain Energy Rev* 2015;44:847–66. <https://doi.org/10.1016/j.rser.2014.12.039>.
- [12] Peng JH; Bi XT; Sokhansanj S; Lim CJ. Torrefaction and densification of different species of softwood residues. *Fuel* 2013;111:411–21. <https://doi.org/10.1016/j.fuel.2013.04.048>.
- [13] Ghiasi B; Kumar L; Furubayashi T; Lim CJ; Bi X; Kim CS; et al. Densified biocoal from woodchips: Is it better to do torrefaction before or after densification? *Appl Energy* 2014;134:133–42. <https://doi.org/10.1016/j.apenergy.2014.07.076>.
- [14] Onyenwoke C; Tabil LG; Mupondwa E; Cree D; Adapa P. Effect of Torrefaction on the Physicochemical Properties of White Spruce Sawdust for Biofuel Production. *Fuels* 2023;4:111–31. <https://doi.org/10.3390/fuels4010008>.
- [15] Stelte W; Clemons C; Holm JK; Sanadi AR; Ahrenfeldt J; Shang L; et al. Pelletizing properties of torrefied spruce. *Biomass Bioenergy* 2011;35:4690–8. <https://doi.org/10.1016/j.biombioe.2011.09.025>.

- [16] Sarker TR; Azargohar R; Dalai AK; Meda V. Enhancement of fuel and physicochemical properties of canola residues via microwave torrefaction. *Energy Rep* 2021;7:6338–53. <https://doi.org/10.1016/j.egy.2021.09.068>.
- [17] Chen C; Yang R; Wang X; Qu B; Zhang M; Ji G; et al. Effect of in-situ torrefaction and densification on the properties of pellets from rice husk and rice straw. *Chemosphere* 2022;289:133009. <https://doi.org/10.1016/j.chemosphere.2021.133009>.
- [18] Grycova B; Klemencova K; Jezerska L; Zidek M; Lestinsky P. Effect of torrefaction on pellet quality parameters. *Biomass Convers Biorefinery* 2022. <https://doi.org/10.1007/s13399-021-02164-8>.
- [19] Igalavithana AD; Mandal S; Niazi NK; Vithanage M; Parikh SJ; Mukome FND; et al. Advances and future directions of biochar characterization methods and applications. *Crit Rev Environ Sci Technol* 2017;47:2275–330. <https://doi.org/10.1080/10643389.2017.1421844>.
- [20] Balogun AO; Lasode OA; McDonald AG. Thermo-physical; Chemical and Structural Modifications in Torrefied Biomass Residues. *Waste Biomass Valorization* 2018;9:131–8. <https://doi.org/10.1007/s12649-016-9787-7>.
- [21] Ong HC; Yu KL; Chen W-H; Pillejera MK; Bi X; Tran K-Q; et al. Variation of lignocellulosic biomass structure from torrefaction: A critical review. *Renew Sustain Energy Rev* 2021;152:111698. <https://doi.org/10.1016/j.rser.2021.111698>.
- [22] Rezaei H. Physical and thermal characterization of ground wood chip and ground wood pellet particles. University of British Columbia; 2017.
- [23] Yu Y; Lau A; Sokhansanj S. Improvement of the pellet quality and fuel characteristics of agricultural residues through mild hydrothermal treatment. *Ind Crops Prod* 2021;169:113654. <https://doi.org/10.1016/j.indcrop.2021.113654>.
- [24] Zheng Y; Tao L; Yang X; Huang Y; Liu C; Gu J; et al. Effect of the Torrefaction Temperature on the Structural Properties and Pyrolysis Behavior of Biomass. *BioResources* 2017;12:3425–47. <https://doi.org/10.15376/biores.12.2.3425-3447>.
- [25] Yang X; Zhao Z; Zhao Y; Xu L; Feng S; Wang Z; et al. Effects of torrefaction pretreatment on fuel quality and combustion characteristics of biomass: A review. *Fuel* 2024;358:130314. <https://doi.org/10.1016/j.fuel.2023.130314>.
- [26] Jaya Shankar Tumuluru; Christopher T Wright; Kevin L Kenney; Richard J Hess. A Technical Review on Biomass Processing: Densification; Preprocessing; Modeling and Optimization. 2010 Pittsburgh Pa. June 20 - June 23 2010; American Society of Agricultural and Biological Engineers; 2010. <https://doi.org/10.13031/2013.29874>.
- [27] Wang Z; Lim CJ; Grace JR; Li H; Parise MR. Effects of temperature and particle size on biomass torrefaction in a slot-rectangular spouted bed reactor. *Bioresour Technol* 2017;244:281–8. <https://doi.org/10.1016/j.biortech.2017.07.097>.
- [28] Li H; Liu X; Legros R; Bi XT; Lim CJ; Sokhansanj S. Torrefaction of sawdust in a fluidized bed reactor. *Bioresour Technol* 2012;103:453–8. <https://doi.org/10.1016/j.biortech.2011.10.009>.
- [29] Yuan H; Yang Q; Wang Y; Gu J; He M; Sun F. Impact of Torrefaction on the Fuel Properties and Combustion Characteristics of Compost of Food Waste and Sawdust. *Energy Fuels* 2018.
- [30] Mafu LD. Structural and chemical modifications of typical South African biomasses during torrefaction. *Bioresour Technol* 2016.
- [31] Wilk M; Magdziarz A; Kalemba I. Characterisation of renewable fuels' torrefaction process with different instrumental techniques. *Energy* 2015;87:259–69. <https://doi.org/10.1016/j.energy.2015.04.073>.
- [32] Ibrahim RHH. Physicochemical characterisation of torrefied biomass. *J Anal Appl Pyrolysis* 2013.
- [33] Gong C. Effects and mechanism of ball milling on torrefaction of pine sawdust. *Bioresour Technol* 2016.
- [34] Neupane S; Adhikari S; Wang Z; Ragauskas AJ; Pu Y. Effect of torrefaction on biomass structure and hydrocarbon production from fast pyrolysis. *Green Chem* 2015.
- [35] Wang S; Dai G; Ru B; Zhao Y; Wang X; Xiao G; et al. Influence of torrefaction on the characteristics and pyrolysis behavior of cellulose. *Energy* 2017;120:864–71. <https://doi.org/10.1016/j.energy.2016.11.135>.
- [36] Chen W-H; Kuo P-C. Torrefaction and co-torrefaction characterization of hemicellulose; cellulose and lignin as well as torrefaction of some basic constituents in biomass. *Energy* 2011;36:803–11. <https://doi.org/10.1016/j.energy.2010.12.036>.